



Plasticized solid polymer electrolyte based on natural polymer blend incorporated with lithium perchlorate for electrical double-layer capacitor fabrication

Y. M. Yusof¹ · M. F. Shukur² · M. H. Hamsan³ · K. Jumbri² · M. F. Z. Kadir⁴

Received: 16 January 2019 / Revised: 2 May 2019 / Accepted: 26 May 2019 / Published online: 8 June 2019
© Springer-Verlag GmbH Germany, part of Springer Nature 2019

Abstract

A plasticized solid polymer electrolyte system is prepared using polymer blend of methyl cellulose–potato starch with lithium perchlorate (LiClO_4) as dopant salt and glycerol as plasticizer. Transport properties of the electrolytes are investigated using electrical impedance spectroscopy (EIS). By applying a method proposed by Arof et al. which was found to be suitable for both Arrhenius and Vogel–Tammann–Fulcher (VTF) type of electrolytes, the number density (n), diffusion coefficient (D), and mobility (μ) of ions are found to be influenced by the concentration of glycerol. From ion and electron transference number analysis, it is verified that ions are the main charge carriers. Linear sweep voltammetry (LSV) verifies the suitability of the most conductive electrolyte to be employed in the carbon-based symmetric electrical double-layer capacitor (EDLC) fabrication. The EDLC has been tested using the galvanostatic charge–discharge and cyclic voltammetry (CV) techniques. The specific capacitance (C_{sp}) of the electrode using CV at a sweep rate of 2 mV s^{-1} is found to be 61.58 F g^{-1} . The EDLC has been tested for 1000 charge–discharge cycles with the highest C_{sp} value of 28.04 F g^{-1} .

Keywords Methyl cellulose–starch blend · Polymer electrolyte · Lithium perchlorate · Transport properties · Electrical double-layer capacitor

Introduction

Numerous reports on liquid electrolytes provide excellent ionic conductivities but facing drawbacks including corrosion, leakage, evaporation, and handling difficulty [1]. Researchers found that solid polymer electrolytes (SPEs) offer advantages by overcoming the problems of using liquid electrolytes. Various efforts have been carried out to improve the performance of SPEs including a polymer blending technique,

which is widely known as an efficient technique to enhance physical and mechanical properties of the electrolytes [2, 3]. In polymer blending, the miscibility of the components is the most important indication as a good polymer electrolyte [4].

High miscibility of methyl cellulose (MC) and potato starch has been proven in our previous work based on thermogravimetric analysis (TGA) and X-ray diffraction (XRD) characterizations [5]. Apart of being non-toxic, biodegradable, and economical, MC possesses high mechanical strength and extraordinary film forming property [6]. Starch is another type of natural polymer which is highly abundant and received wide attention due to availability, inexpensiveness, and easy degradability [7]. However, the electrolytes produced from starch are brittle and sensitive to moisture [8]. Blending starch with MC has resulted in improved electrical, physical, and mechanical properties [5]. This improvement will be further investigated based on electrical double-layer capacitor (EDLC) performance using MC–starch– LiClO_4 –glycerol electrolyte.

The addition of LiClO_4 salt as an ion provider has enhanced the amorphous region which is important in supporting the segmental motions and further increased the

✉ M. F. Shukur
mfadhullah.ashukur@utp.edu.my

¹ Universiti Kuala Lumpur Malaysian Institute of Chemical and Bio-Engineering Technology, Alor Gajah, 78000 Malacca, Malaysia

² Fundamental and Applied Sciences Department, Universiti Teknologi PETRONAS, 32610 Seri Iskandar, Malaysia

³ Institute of Graduate Studies, University of Malaya, 50603 Kuala Lumpur, Malaysia

⁴ Centre for Foundation Studies in Science, University of Malaya, 50603 Kuala Lumpur, Malaysia

ion conductivity subsequently [9]. High diffusion rate due to large size of ClO_4^- anion and small size of Li^+ cation with low lattice energy of LiClO_4 contributes to the increment of ionic conductivity [5]. The amorphous region was further enhanced by the addition of glycerol as plasticizer which also can improve the electrochemical and mechanical properties of electrolytes [10]. To our best knowledge, no report has been found on the fabrication of supercapacitor using polymer electrolyte based on MC–potato starch blend incorporated with LiClO_4 .

Supercapacitor is a promising candidate for charge storage devices due to extensive life cycle and excellent power density compared with rechargeable batteries [11, 12]. Supercapacitors can be combined with fuel cells/batteries in vehicles with a hybrid system to provide high power density throughout speeding and regain energy while braking [13]. Supercapacitors are divided into two types depending on the mechanisms of charge storage: EDLCs with reversible adsorption of ions on the electrode and electrolyte interfaces and pseudocapacitors (PCs) where the surface of electrodes undergoes fast redox reactions [14].

An EDLC consists of two porous electrodes, where the electrolyte which possesses a high ionic conductivity with promising electrochemical window along with good thermal and mechanical stability is sandwiched between the electrodes [1, 7]. The energy in EDLC is stored by charge separation in Helmholtz double layers across the blocking electrode–electrolyte interfaces due to electrostatic interactions between the ions in the electrolyte with the active electrode materials [15]. Compared with batteries, EDLC is more environmentally friendly with high power density, longer lifetime, and high cyclability [16, 17].

Our previous work shows that the MC–starch– LiClO_4 system possesses the highest room temperature conductivity of $(4.25 \pm 0.82) \times 10^{-4} \text{ S cm}^{-1}$ when added with 20 wt% of glycerol [5]. In this work, further characterization of electrochemical properties and EDLC fabrication have been carried out to prove that this system has a big potential in supercapacitor application. We use a method proposed by Arof et al. [18] to assess the transport properties of the electrolytes. Compared with the Rice and Roth model [19], this method can be used regardless of the type of electrolyte, whether the electrolytes obey Arrhenius or Vogel–Tammann–Fulcher (VTF) rules.

Experimental

Electrolytes preparation

A 0.4 g of potato starch (Sigma-Aldrich) was dissolved in 100 mL of 1% acetic acid (SYSTEM) and stirred at 80 °C for 20 min. After the solution was cooled to room temperature, 0.6 g of MC was added to the starch solution. The starch–MC

mixtures were stirred until the solutions become homogeneous. Then, 0.25 g of LiClO_4 (Sigma-Aldrich) was added to the polymer blend solutions and stirred until homogeneous solutions have been obtained. Desired amounts of glycerol (SYSTEM) were then added and stirred until complete dissolution. All solutions were cast into different plastic Petri dishes and left to dry for 2–3 days at room temperature. The dried films were then kept in a desiccator filled with silica gel desiccants for further drying to avoid any trace moisture. Table 1 shows the designations and compositions of each plasticized electrolyte.

Electrical impedance spectroscopy

Electrolytes were placed in between stainless steel blocking disc electrodes and held under spring pressure. The impedance analyses of the electrolytes were performed in a range of frequencies from 50 Hz to 5 MHz at room temperature (25 °C, RH ~ 50%) using an LCR meter (HIOKI 3532-50).

Transference number measurements

Ionic transference number (t_{ion}) was obtained using the dc polarization method [20]. Polarization of a cell consisting of an electrolyte and stainless steel electrodes was carried out at room temperature using V&A Instrument DP3003 at a potential of 0.030 V. The dc current was monitored as a function of time.

Voltammetry analysis

Linear sweep voltammetry (LSV) was conducted using DIGIVY DY2300 potentiostat to evaluate the electrochemical stability of the plasticized electrolyte at room temperature. Stainless steel was employed as counter, reference, and working electrodes. LSV analysis was done at a sweep rate of 5 mV s^{-1} from 0 to 2.5 V.

Carbon-based electrode preparation

A mixture of 6.25 wt% carbon black (Super P), 12.5 wt% polyvinylidene fluoride (PVdF), and 81.25 wt% activated carbon (RP20) was stirred in N-methylpyrrolidone (NMP) (EMPLURA) to prepare the electrode slurry. An aluminum foil, which serves as the current collector, was then coated with the slurry of 0.25-mm thickness and dried at 60 °C. The electrode thickness was reduced to 0.10 mm after the drying process.

Characterization using EDLC

The EDLC was constructed by employing the highest conducting electrolyte to separate the identical carbon-based

Table 1 Composition and designation of electrolytes

Designation	Composition of MC–starch–LiClO ₄ –glycerol					
	Weight of MC–starch–LiClO ₄ (g)			Weight percentage of MC–starch–LiClO ₄ (wt%)	Weight of glycerol (g)	Weight percentage of glycerol (wt%)
	MC	Starch	LiClO ₄			
A5	0.600	0.400	0.250	95	0.066	5
A10	0.600	0.400	0.250	90	0.139	10
A15	0.600	0.400	0.250	85	0.221	15
A20	0.600	0.400	0.250	80	0.313	20
A25	0.600	0.400	0.250	75	0.417	25
A30	0.600	0.400	0.250	70	0.536	30

electrodes. The EDLC cell was clamped between two Perspex plates for characterization purpose. Cyclic voltammetry (CV) measurements were conducted using Digi-IVY DY2300 potentiostat in the voltage range of 0 to 1.0 V with varied sweep rates. The measurements were done at room temperature. Cyclability of the EDLC was tested using Neware battery cycle at a constant current of 0.13 mA.

Results and discussion

Transport analysis

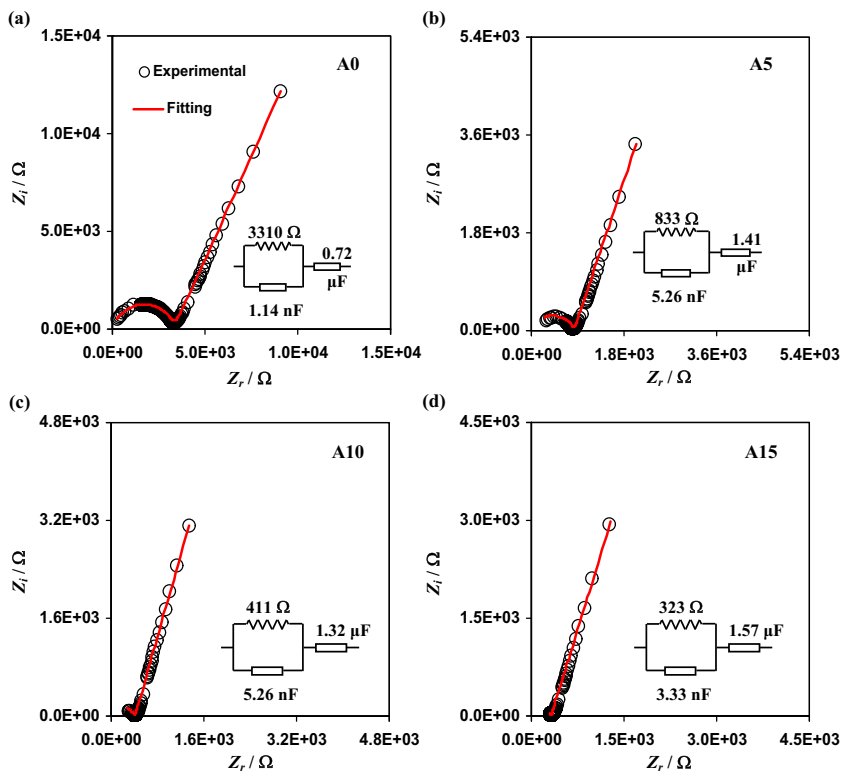
Electrical impedance spectroscopy (EIS) is well-known as an excellent and nondestructive technique to be used in polymer electrolytes studies. In this work, the EIS technique was performed to study the electrical characteristic of methyl cellulose–potato starch blend-based electrolytes. Figure 1 shows the room temperature Nyquist plots for A0, A5, A10, and A15. The Nyquist plot of A0 in Fig. 1a possesses a tilted spike at the low-frequency region and semicircular arc at the high-frequency region. The semicircle curve is corresponded to the conduction of charges in the bulk of the electrolyte [21]. Based on a report by Malathi et al. [22], the parallel combination of bulk capacitance and resistance of the polymer electrolytes leads to the bulk conductivity. The tilted spike represents the polarization of electrode that is a feature of diffusion mechanism [21]. The angle of the tilted spikes is smaller than 90° with respect to the real axis. This kind of impedance plot is due to electrode–electrolyte interface inconsistent structure [23, 24]. The electrode–electrolyte interface could be regarded as a capacitance because the stainless steel electrodes have been employed in the EIS analysis [25]. The semicircle part is observed to be diminished when the glycerol content rises to 15 wt%. The value of bulk resistance (R_b) is obtained at the intercept of tilted spike and the semicircle. The semicircle part completely disappears and leaving only a single tilted spike as 20 wt% glycerol is added (i.e., A20) as depicted in Fig. 2a.

The absence of semicircle illustrates the existent of resistive part of the electrolyte [26]. The R_b value is extracted from the intercept of the horizontal axis with tilted spike. The R_b value decreases as the amount of glycerol increases to 20 wt%. It is due to the increase in the number of mobile ions when more plasticizers were added [27, 28]. The high dielectric constant value of the plasticizer can weaken the forces between the anions and cations of the LiClO₄ salt and simultaneously create more pathways for ion conduction [5]. Nevertheless, the addition of more than 20 wt% glycerol leads to the formation of microcrystalline junctions between the plasticizer molecules, hence reducing the conductivity.

Starch consists of repeating 1,4- α -D-glucopyranosyl units, which are amylose and amylopectin [5]. Amylopectin consists of short chains of double helices packed arrangement which mainly contributes to crystallinity of starch. These stacked lamellae can be observed by the microscopic techniques with ~ 10 to 500 nm in thickness [29]. Cellulose is a polysaccharide consisting of linear chains of β (1–4) glucosidic units [6]. A slight helical twist exists primarily due to intramolecular hydrogen bonding between the hydroxyl group on C-3 and the pyranose ring oxygen in the adjoining glucose monomers and also between the hydroxyl groups on C-6 and C-2 of the adjacent glucose units. These intramolecular bonding contribute to the rigidity of the cellulose molecules, particularly in solid cellulose. The hydroxyl groups have high tendency to form intermolecular hydrogen bonds between neighboring cellulose chains resulting the formation of crystallite strands, which referred as highly ordered microcrystalline structures [29].

In the present work, MC and starch are blended, followed by the addition of LiClO₄ as ion provider and glycerol as plasticizer. However, excess glycerol will lead to conductivity decrement as well as decreasing the mechanical properties of the film [15]. The intermolecular interactions among the plasticizer molecules and intramolecular interaction between molecules of polymer host, salt, and the plasticizer molecules might take place when the ions and molecules become too

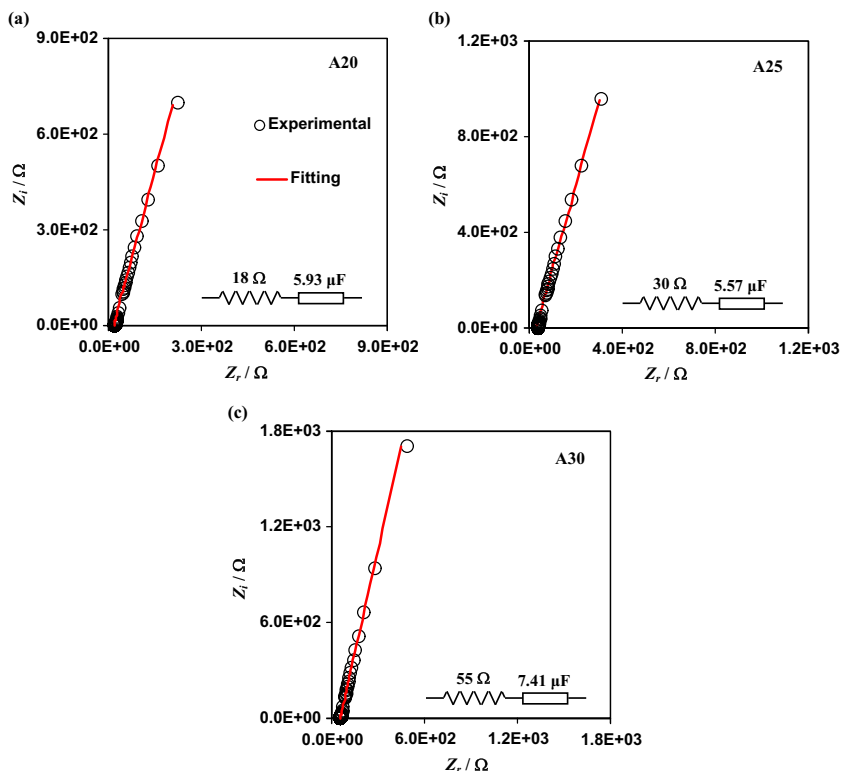
Fig. 1 Nyquist plot and the corresponding fitting curve for **a** A0, **b** A5, **c** A10, and **d** A15. The inset figure shows the corresponding equivalent circuit



close, which further enhance the crystalline regions and may occur at micro level of the molecule units. This characteristic can be confirmed by X-ray diffraction (XRD) analysis, which exhibited in [5].

The polymer electrolytes in this work are Arrhenian since the regression value (R^2) of conductivity–temperature plot is nearly 1 [5]. Basically, conductivity (σ) of polymer electrolytes can be expressed as follows:

Fig. 2 Nyquist plot and the corresponding fitting curve for **a** A20, **b** A25, and **c** A30. The inset figure shows the corresponding equivalent circuit



$$\sigma = \mu ne \tag{1}$$

where μ is the ionic mobility, n is the number density of free ions that contributes to conductivity, and e is elementary charge. Based on Eq. (1), it can be observed that μ and n are two significant parameters that crucial in determining conductivity values of electrolyte. Hence, it will be convenient if μ and n can be obtained quantitatively. Using a method proposed by Arof et al. [18], the two parameters can be evaluated by fitting the impedance curve. As the impedance data of A0, A5, A10, and A15 consist of a tilted spike and a semicircle, the equivalent model can be portrayed by a parallel arrangement of a constant phase element (CPE) and a resistor which is connected with another CPE in series as shown in the inset of all Nyquist plots in Fig. 1 [30]. The imaginary and real parts of impedance, Z_i and Z_r , respectively, of the equivalent model in the inset of Fig. 1 are given by the following equations [6]:

$$Z_r = \frac{R_b + R_b^2 C_1 \omega^{p_1} \cos\left(\frac{\pi p_1}{2}\right)}{1 + 2R_b C_1 \omega^{p_1} \cos\left(\frac{\pi p_1}{2}\right) + R_b^2 C_1^2 \omega^{2p_1}} + \frac{\cos\left(\frac{\pi p_2}{2}\right)}{C_2 \omega^{p_2}} \tag{2}$$

$$Z_i = \frac{R_b^2 C_1 \omega^{p_1} \sin\left(\frac{\pi p_1}{2}\right)}{1 + 2R_b C_1 \omega^{p_1} \cos\left(\frac{\pi p_1}{2}\right) + R_b^2 C_1^2 \omega^{2p_1}} + \frac{\sin\left(\frac{\pi p_2}{2}\right)}{C_2 \omega^{p_2}} \tag{3}$$

where C_1 is the capacitance at high frequency, C_2 is the capacitance at low frequency, ω is angular frequency, p_2 is the deviation of the tilted spike from the horizontal axis, and p_1 is the deviation of the circle radius from the vertical axis. The value of μ can be acquired from the given equation:

$$\mu = \frac{eD}{k_B T} \tag{4}$$

where T is the absolute temperature and k_B is the Boltzmann constant. The method by Arof et al. [18] describes diffusion coefficient (D) via the following equation:

$$D = \frac{(k_2 \varepsilon_o \varepsilon_r A)^2}{\tau_2} \tag{5}$$

where ε_r is the dielectric constant, ε_o is the vacuum permittivity, and k_2 is the inverse of capacitance C_2 . C_2 is the capacitance due to the double-layer formation at the electrode–

electrolyte interface throughout the impedance analysis. τ_2 is the inverse of angular frequency corresponding to the minimum in Z_i . According to a report by Fadzallah et al. [30], a constant value of $\log \varepsilon_r$ should be taken. From our previous report [5], the ε_r values for MC–starch–LiClO₄–glycerol electrolytes were almost constant at $\log f > 5$. Thus, the ε_r values at $\log f > 5$ have been chosen for A0, A5, A10, and A15. Table 2 provides the values of p_2 , ε_r , k_2 , and τ_2 for A5, A10, and A15 electrolytes.

The Nyquist plots of A20, A25, and A30 consist of only a tilted spike. Thus, the equivalent model can be portrayed by a series combination of a CPE and a resistor as shown in the inset of all Nyquist plots in Fig. 2 [31]. The values of Z_r and Z_i associated to the equivalent model in the inset of Fig. 2 can be described as follows:

$$Z_r = R_b + \frac{\cos\left(\frac{\pi p}{2}\right)}{C \omega^p} \tag{6}$$

$$Z_i = \frac{\sin\left(\frac{\pi p}{2}\right)}{C \omega^p} \tag{7}$$

where p is the deviation of the tilted spike from the horizontal axis and C represents the capacitance of CPE. The values of D for A20, A25, and A30 are determined using the following equation [32, 33]:

$$D = D_o \exp\left\{-0.0297[\ln D_o]^2 - 1.4348[\ln D_o] - 14.504\right\}. \tag{8}$$

where

$$D_o = \frac{4k^4 l^2}{R_b^4 \omega_{\min}^3} \tag{9}$$

Here l is the thickness of the electrolyte, ω_{\min} is the angular frequency corresponding to the minimum Z_i , and k is the inverse of C . The n and μ for A20, A25, and A30 can be calculated using Eqs. (1) and (4), respectively. Table 3 lists the values of p , k , and ω_{\min} for A20, A25, and A30.

Table 2 The values of p_2 , k_2 , ε_r , and τ_2 for A5, A10, and A15 at room temperature

Sample	p_2	$k_2 (\times 10^5 \text{ F}^{-1})$	ε_r	$\tau_2 (\times 10^{-7} \text{ s})$
A5	0.783 ± 0.005	7.08 ± 1.82	4.56 ± 1.41	16.55 ± 1.83
A10	0.788 ± 0.009	7.57 ± 0.91	4.70 ± 0.82	10.78 ± 3.79
A15	0.809 ± 0.005	6.38 ± 0.69	5.37 ± 2.12	6.50 ± 2.06

Figure 3 shows the variations of D , μ , and n of charge carriers against glycerol content for MC–starch-based electrolytes. Based on Fig. 3a, the value of D is observed to rise gradually from $(1.94 \pm 0.60) \times 10^{-7} \text{ cm}^2 \text{ s}^{-1}$ to $(1.50 \pm 0.32) \times 10^{-6} \text{ cm}^2 \text{ s}^{-1}$ when the concentration of glycerol increases from 5 to 20 wt%. The similar trend is shown by μ as depicted in Fig. 3b where μ value increases from $(7.70 \pm 2.31) \times 10^{-6} \text{ cm}^2 \text{ V}^{-1} \text{ s}^{-1}$ (A5) to $(5.86 \pm 1.24) \times 10^{-5} \text{ cm}^2 \text{ V}^{-1} \text{ s}^{-1}$ (A20). The increase in μ and D can be attributed to the enhancement of chain flexibility in MC–starch polymer blend host with the presence of glycerol [31]. When the concentration of glycerol is beyond 20 wt%, the values of D and μ are reduced which lead to conductivity decrement [5]. The value of n increases as the glycerol content increases to 30 wt% as shown in Fig. 3c. This is because the inclusion of excess glycerol in the MC–starch-based electrolytes dissociates more salts into free ions, hence increasing the number density of charge carriers. However, beyond 20 wt% glycerol content, too much ions are provided; thus, the collisions among free ions can solely take place. This condition provides limited space for the ions to move around, hence decreasing their mobility and diffusivity [32].

In Fig. 3, μ and n of charge carriers for A5, A10, and A15 were determined by calculating D using Eq. (5). For A20, A25, and A30, D was calculated using Eq. (8) to determine μ and n . For comparison purposes, μ and n of charge carriers for A5, A10, and A15 were recalculated using Eq. (8). The variations of D , μ , and n of charge carriers against glycerol content have been replotted as shown in Fig. 4. It is found that D increases from $(2.21 \pm 0.60) \times 10^{-9} \text{ cm}^2 \text{ s}^{-1}$ to $(1.02 \pm 6.36) \times 10^{-7} \text{ cm}^2 \text{ s}^{-1}$ as glycerol varies from 5 to 15 wt%, respectively. μ and n for the electrolyte with 15 wt% glycerol are $(2.36 \pm 0.34) \times 10^{-6} \text{ cm}^2 \text{ V}^{-1} \text{ s}^{-1}$ and $(4.84 \pm 1.29) \times 10^{19} \text{ cm}^{-3}$, respectively. Due to different approaches, the values of D , μ , and n are expected to be different when using Eq. (8). By comparing the values of D , μ , and n of A5, A10, and A15 obtained in Figs. 3 and 4, the values are not close to each other. However, the parameters in Fig. 4 still follow the same trend as in Fig. 3. Thus, the pattern of the conductivity has further strengthened with this transport parameters.

Transference number of selected plasticized electrolytes was measured to determine the main conducting species in the electrolytes. Electrons can pass through the stainless steel (SS) electrodes; hence, a cell arrangement of SS/

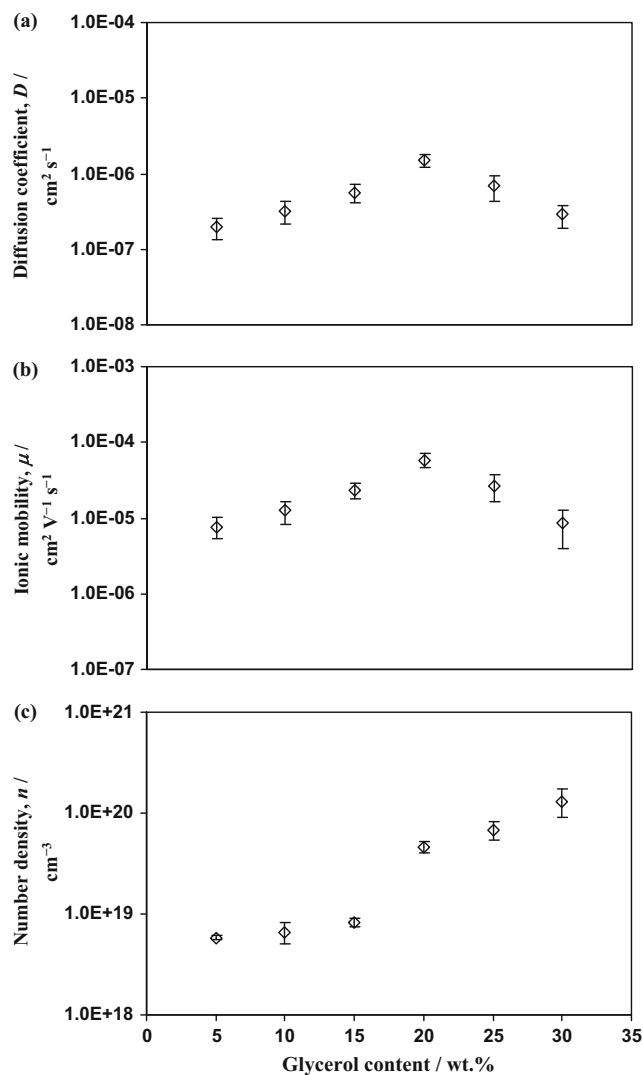


Fig. 3 Plot of **a** diffusion coefficient (D), **b** mobility (μ), and **c** number density (n) of ions against glycerol content using Eqs. (5) and (8)

electrolyte/SS was constructed [34]. The cell was polarized at 0.03 V, and the potentiostatic current versus time was recorded for A15, A20, and A25, as shown in Fig. 5. An ionic conductor will show an abrupt fall in the current flow at the beginning of the polarization before reaching a constant value. The plots in Fig. 5 show constant reading at 0.1 μA indicating the steady-state current. This result is comparable with the work reported by Kufian et al. [34] with applied voltage of 0.08 V using Wagner's polarization technique for the Li-ion-based electrolyte system. The initial current is high due to the migration of ions and electrons, before the ion movement is blocked at the electrode–electrolyte interface. The polarization current starts to drop with time since only electrons could pass through the electrodes [35]. Therefore, the steady state is obtained only due to electrons [36]. The transference numbers of ion (t_{ion}) and electron (t_{elec}) are calculated using the following equations:

Table 3 The values of p , k , and ω_{min} for A20, A25, and A30 at room temperature

Sample	p	$k (\times 10^5 \text{ F}^{-1})$	$\omega_{\text{min}} (\times 10^6 \text{ rad s}^{-1})$
A20	0.831 ± 0.002	1.69 ± 0.21	1.04 ± 0.07
A25	0.823 ± 0.007	1.80 ± 0.22	1.23 ± 0.21
A30	0.834 ± 0.006	1.35 ± 0.18	1.07 ± 0.18

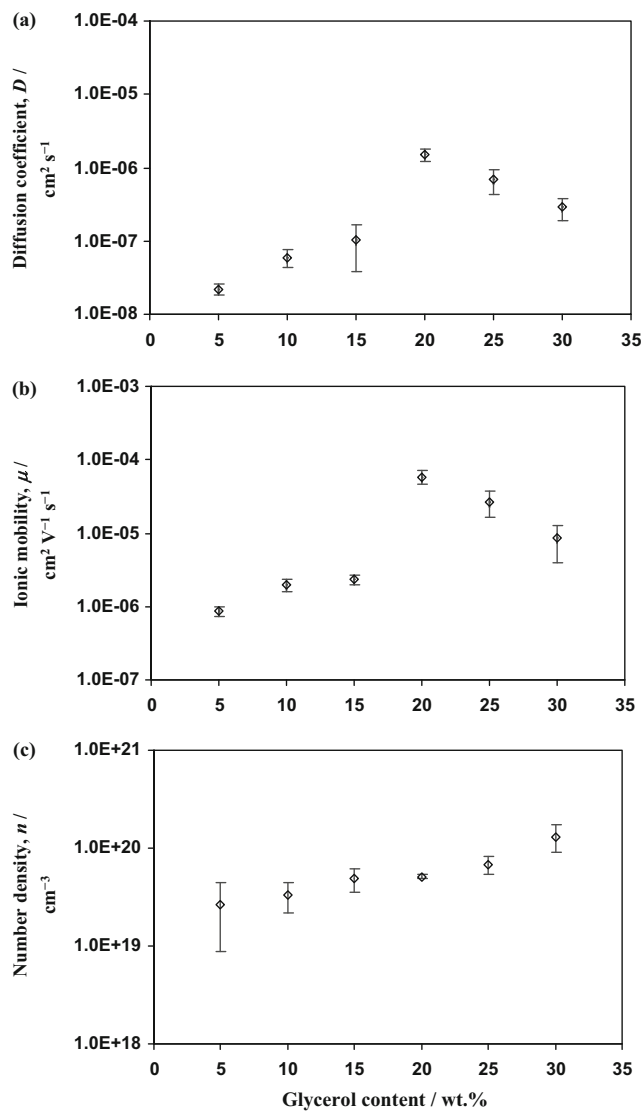


Fig. 4 Plot of **a** diffusion coefficient (D), **b** mobility (μ), and **c** number density (n) of ions against glycerol content using Eq. (8)

$$t_{\text{ion}} = \frac{(I_i - I_f)}{I_i} \tag{10}$$

$$t_{\text{elec}} = \frac{I_f}{I_i} \tag{11}$$

where I_f is the final residual current and I_i is the initial current. The values are presented in Table 4. The values are almost unity signifying that these electrolytes are ionic conductors [37]. The trend in t_{ion} follows the D and μ trends as shown in Figs. 3 and 4 which signifies the ionic conductivity trend for the plasticized system. The contribution of ionic current in the total conductivity is very significant since the ions, which are the charge carriers, play important roles in device application. The high t_{ion} at low dc voltage strongly proves a stable ionic conduction and an excellent indication for a good device performance. Jinisha et al. [37] reported that their polymer blend

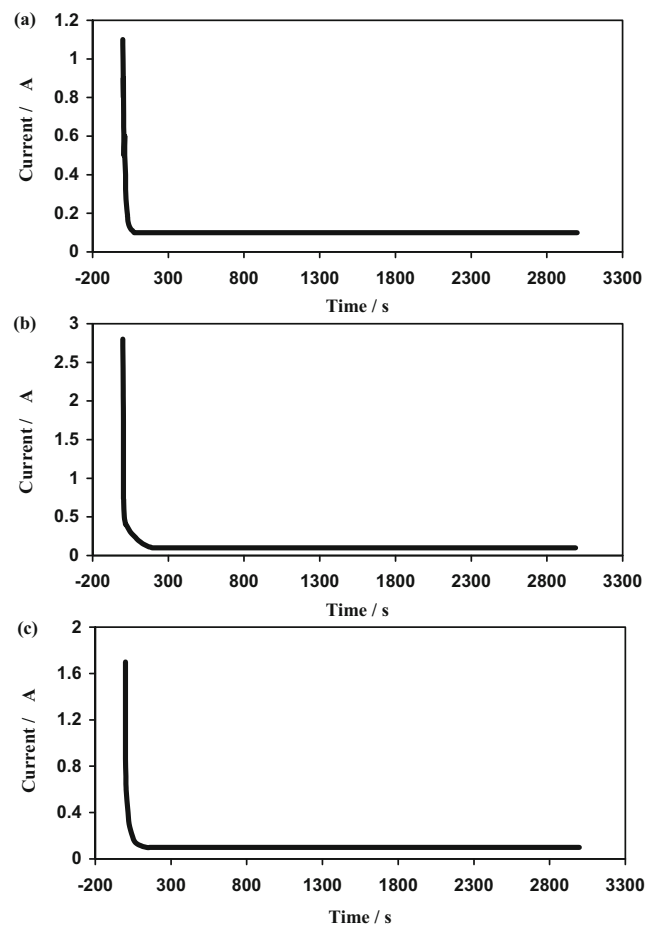


Fig. 5 Ionic transference number for **a** A15, **b** A20, and **c** A25 using 30 mV dc bias voltage

electrolytes based on polyvinyl pyrrolidone (PVP)/polyethylene oxide (PEO) infused with lithium nitrate (LiNO_3) exhibited the highest conductivity of $1.13 \times 10^{-3} \text{ S cm}^{-1}$, which assembled the highest t_{ion} of 0.9997 under a fixed dc voltage of 0.5 V. Hu et al. [36] obtained t_{ion} in the range of 0.98–0.99 for the electrolytes based on the lithium bis(trifluoromethanesulfonyl)imide (LiTFSI) salt as the dopant and poly(diallyldimethylammonium)bis(trifluoromethanesulfonyl)imide (poly(DADMATFSI)) under a dc voltage of 1 V. These reports are comparable with the present results which indicate that the MC–starch-based electrolytes are good ionic conductors and particularly proven when the lower dc voltage of 0.03 V is used during polarization.

Table 4 Ionic and electronic transference numbers of selected electrolytes

Sample	t_{elec}	t_{ion}
A15	0.09	0.91
A20	0.04	0.96
A25	0.06	0.94

LSV analysis

Linear sweep voltammetry (LSV) has been conducted to examine the electrochemical stability and the capability of the polymer electrolytes to persist the working voltage during fabrication of electrochemical devices [38]. Figure 6 depicts the LSV voltammogram of the electrolyte with the highest conductivity which operated at 5 mV s^{-1} where stainless steel is employed as counter, reference, and working electrodes. It is noticeable from the curve that the plateau is flat and straight at the beginning. As the voltage is swept towards positive values, the current increases significantly due to electrolyte decomposition and marking a breakdown voltage at $\sim 2.0 \text{ V}$. In [9], the sample with the highest conductivity in the starch–lithium acetate–glycerol system possesses decomposition voltage at 2.1 V (sweep rate = 5 mV s^{-1}). This result verifies that electrolyte with the highest conductivity in this work is electrochemically stable up to 2.0 V ; hence, it is suitable for EDLC application.

EDLC characterization

To understand the potential of MC–starch-based polymer electrolytes for device application, an EDLC has been fabricated by placing A20 electrolyte between carbon electrodes. The performance of the EDLC was analyzed using CV at various sweep rates from 0 to 1.0 V at room temperature. From Fig. 7, the cyclic voltammogram of the EDLC shows almost a rectangular shape at sweep rate of 2 mV s^{-1} . The divergence from the rectangular shape when the sweep rate increases can be attributed to the porous structure, and resistance of carbon consequently creates a current dependence of voltage [39]. At 2 mV s^{-1} sweep rate, the rectangular shape of CV plot which possesses almost a mirror image of the current responses about the zero current line indicates the capacitive behavior of the EDLC with double-layer development on the surfaces [40]. The values of specific capacitance (C_{sp}) of electrode at various sweep rates are calculated using the following equation:

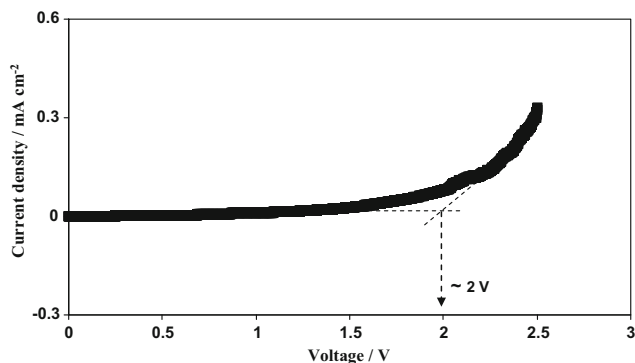


Fig. 6 LSV for the highest conducting electrolyte at 5 mV s^{-1}

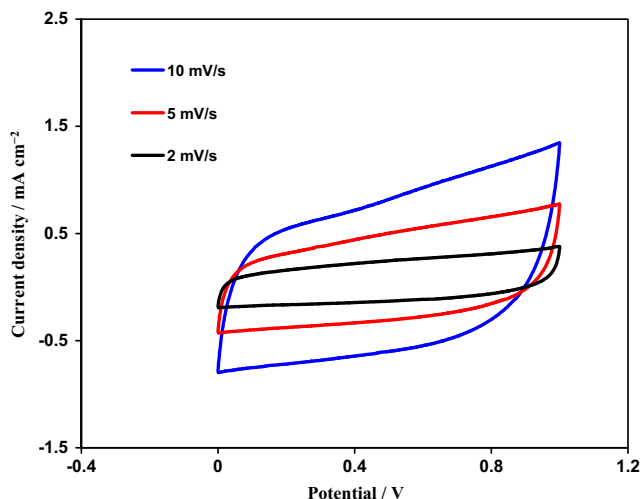


Fig. 7 Cyclic voltammogram of EDLC at different sweep rates

$$C_{\text{sp}} = \frac{4}{(V_f - V_i) M \nu} \int_{V_i}^{V_f} I(V) dV \quad (12)$$

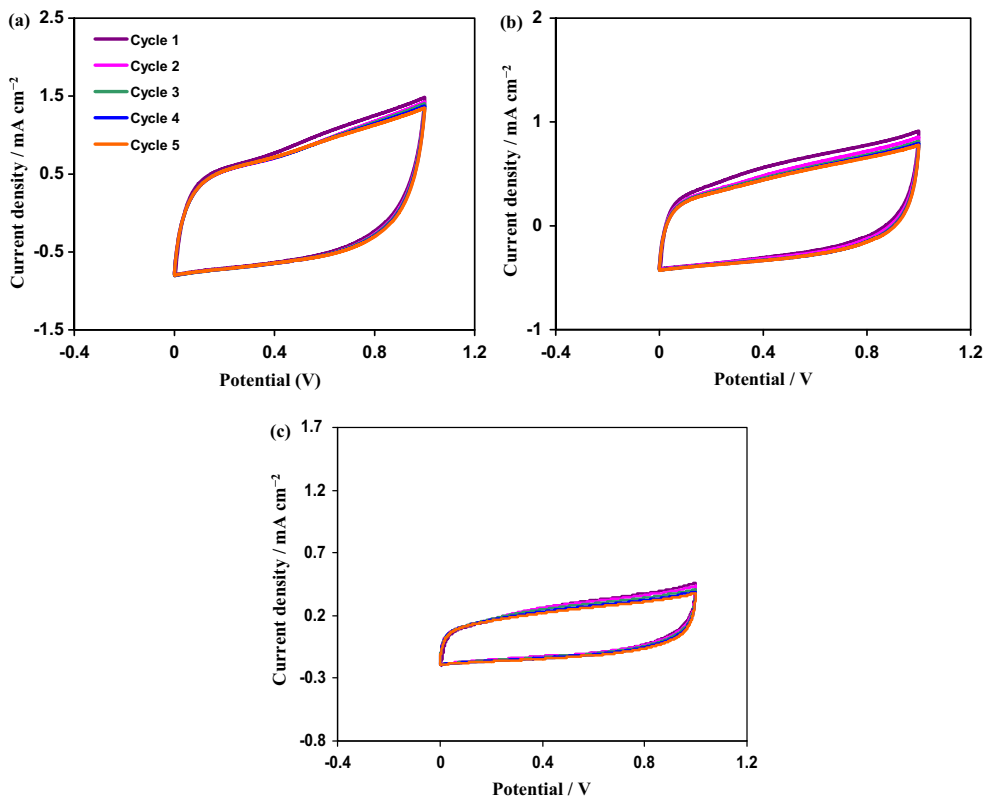
where $\int I(V) dV$ stands for area of the cyclic voltammogram, $(V_f - V_i)$ represents the potential window, ν is the applied sweep rate, while M stands for mass of active material in both electrodes. The C_{sp} at different sweep rates are listed in Table 5 with sweep rate of 2 mV s^{-1} produced the highest C_{sp} of 61.58 F g^{-1} . It is obvious that the C_{sp} value reduces as the sweep rate increases. As the sweep rate increases, the number of stored charges on the electrode surface is reduced, and energy loss increases leading to a decrease in C_{sp} [41, 42]. Ions could reach the electro-active sites adequately at slow scan rate leading to the increase in C_{sp} [43]. Liew and Ramesh [44] reported the EDLC with activated carbon electrode and corn starch– LiPF_6 – BmImPF_6 electrolyte exhibits specific capacitance of 36.79 F g^{-1} at 10 mV s^{-1} . Shukur et al. [9] reported specific capacitance of EDLC with activated carbon electrodes and starch– LiOAc –glycerol at 10 to 0.5 mV s^{-1} is in the range from 23.39 to 33.00 F g^{-1} .

The cyclic stability of the EDLC was also examined using CV. The cyclic stability of the EDLC was measured for 5 cycles. As seen in Fig. 8, the device exhibits good cyclic stability with no sign of degradation in the charge storage capacity at all sweep rates. The specific capacitance (C_{sp}) of electrode against the cycle number is revealed in Fig. 9. It can

Table 5 Specific capacitance of electrode using CV at different sweep rates

Sweep rates (mV s^{-1})	C_{sp} (F g^{-1})
10	45.82
5	52.57
2	61.58

Fig. 8 Cyclic voltammogram of EDLC at different cycles with sweep rate of **a** 10 mV s⁻¹, **b** 5 mV s⁻¹, and **c** 2 mV s⁻¹



be observed that the C_{sp} values are stable during all cycles. This is a confirmation to illustrate the capability of the EDLC to maintain with continuous cycling, therefore proving a consistent performance in long lifetime [45].

The kinetic parameters acquired from CV plots must follow the law of power with the following equation [46–48]:

$$i = av^b \tag{13}$$

where v represents for the sweep rate, a and b are coefficients, and i stands for the peak current. While $b = 1$ corresponds to capacitive behavior, $b = 0.5$ stands for a semi-infinite diffusion-controlled process. The obtained b value can be used to differentiate the process of storing charge if it arises from diffusion-controlled or capacitive processes. By plotting a $\log(\text{current}) - \log(\text{scan rate})$ plot as observed in Fig. 10, b value of 0.94 is achieved, which signifies that the charge storage is due to charge accumulation at the electrode–electrolyte interface [47].

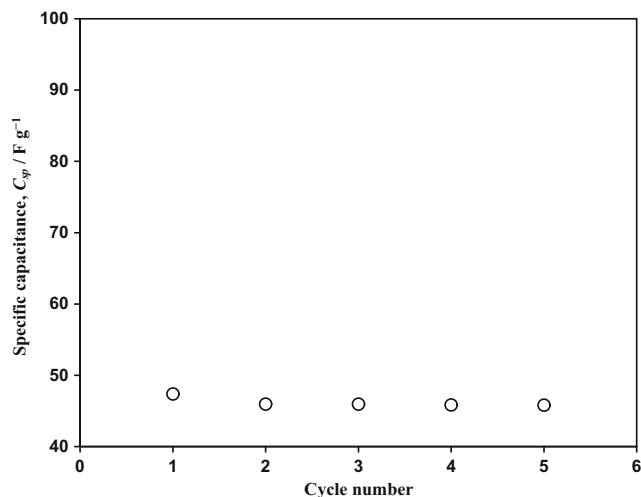


Fig. 9 Variation of C_{sp} of single electrode against cycle number at 10 mV s⁻¹

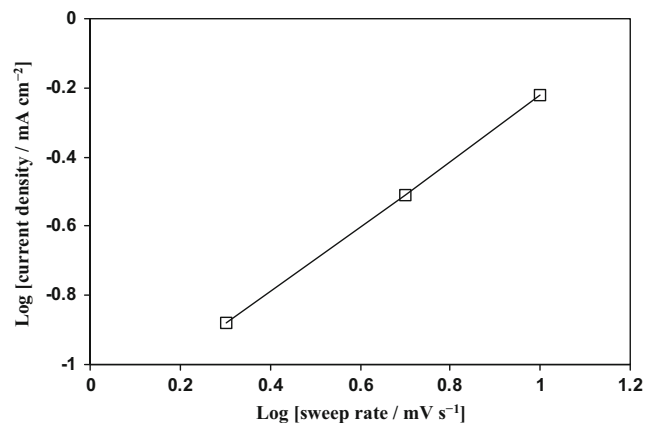


Fig. 10 Log (discharge current density) versus log (sweep rate) plot obtained using discharge current densities at 0.5 V from the CV curves at different sweep rates

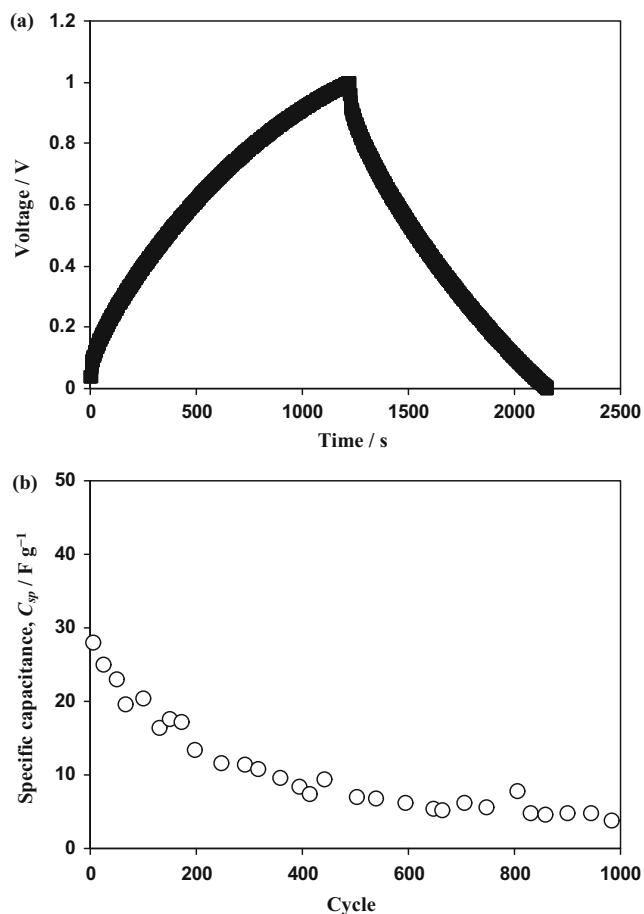


Fig. 11 **a** Typical charge–discharge curve of the EDLC at constant current of 0.13 mA. **b** Specific capacitance against cycle number

Galvanostatic cycling experiments were undertaken to examine the EDLC cycling stability. Figure 11a illustrates the typical charge–discharge plot of EDLC from 0 to 1.0 V. After discharging process, the drastic voltage drop is due to the internal resistance developed from the inter-fluid resistance between the electrolyte and current collector [48]. The C_{sp} of a single electrode can be obtained via the following equation [49]:

$$C_{sp} = 4C \quad (14)$$

Table 6 Specific capacitance of EDLC using lithium-based polymer electrolytes and activated carbon electrodes

Samples	Specific capacitance ($F\ g^{-1}$)	Charge–discharge cycles	References
PMMA–LiBOB	0.521	50	[49]
Com starch–LiClO ₄	7.09	500	[51]
PVA–LiClO ₄	3.0	200	[52]

Here, C represents the specific capacitance for a symmetric cell. For a symmetric EDLC, a linear charge–discharge curve is expected. The following equation is commonly used to determine C :

$$C = \frac{I}{Ms} \quad (15)$$

where I represents the constant current while s stands for the discharge curve slope. However, for a non-perfect linear curve, the above equation will give an overestimated value. Thus, the integral of discharge curve will be used instead of the slope to get an accurate C_{sp} value as shown as follows [50]:

$$C = \frac{2I}{M} \left(\frac{\int_{t_i}^{t_f} V(t) dt}{V^2|_{V_i}^{V_f}} \right) \quad (16)$$

Here, V is the potential with the final and initial values of V_f and V_i , respectively, and $\int V(t) dt$ is the area under the discharge curve. The trend in C_{sp} values for 1000 cycles is depicted in Fig. 11b. The C_{sp} values are reduced as the cycle number increased due to the imperfection of the electrode–electrolyte contact [15]. The highest value of C_{sp} obtained is $28.04\ F\ g^{-1}$ before being almost constant at $\sim 5\ F\ g^{-1}$ due to the stabilization of the ion accumulation at the electrode–electrolyte interface. The performance of activated carbon-based EDLC using other lithium-based polymer electrolytes employing the galvanostatic cycling technique is tabulated in Table 6. It implies that the present electrolyte system is a promising material as an electrolyte in EDLC application.

Conclusions

A polymer electrolyte system based on MC–starch blend infused with LiClO₄ and glycerol as plasticizer was prepared employing a solution cast technique. EIS analysis was performed to analyze the electrical behavior of the electrolytes. The values of D and μ were observed to increase gradually from $(1.94 \pm 0.60) \times 10^{-7}\ cm^2\ s^{-1}$ (A5) to $(1.50 \pm 0.32) \times 10^{-6}\ cm^2\ s^{-1}$ (A20) and from $(7.70 \pm 2.31) \times 10^{-6}\ cm^2\ V^{-1}\ s^{-1}$ (A5) to $(5.86 \pm 1.24) \times 10^{-5}\ cm^2\ V^{-1}\ s^{-1}$ (A20), respectively. The increment in these two parameters can be attributed to the enhancement of chain flexibility in MC–starch–LiClO₄ electrolyte with the presence of glycerol. The values of t_{ion} for A15, A20, and A25 are 0.91, 0.96, and 0.94, respectively, indicating that the polymer electrolytes are ionic conductors. LSV result verifies that electrolyte with the highest conductivity (A20) is electrochemically stable up to 2.0 V and acceptable for EDLC fabrication. CV analysis has

confirmed the capacitive behavior of the EDLC with specific capacitance (C_{sp}) value of 61.58 F g^{-1} at a sweep rate of 2 mV s^{-1} . The C_{sp} was found stable at sweep rates of 10 mV s^{-1} , 5 mV s^{-1} , and 2 mV s^{-1} during the 5 cycles which demonstrates the long lifetime of the device with consistent performance. The EDLC has been tested for 1000 cycles with the highest C_{sp} value of 28.04 F g^{-1} .

Funding information The authors would like to thank the Universiti Teknologi PETRONAS for supporting this work through YUTP grant (grant no. 015LC0-048) and Ministry of Education for Fundamental Research Grant Scheme (FRGS/1/2018/STG07/UNIKL/02/8).

References

- Das S, Ghosh A (2017) Solid polymer electrolyte based on PVDF-HFP and ionic liquid embedded with TiO_2 nanoparticle for electric double layer capacitor (EDLC) application. *J Electrochem Soc* 164: F1348–F1353
- De Kruijff C, Tuinier R (2001) Polysaccharide protein interactions. *Food Hydrocoll* 15:555–563
- Elgadir MA, Akanda MJH, Ferdosh S, Mehrmouh A, Karim AA, Noda T, Sarker MZI (2012) Mixed biopolymer systems based on starch. *Molecules* 17:584–597
- Rajendran S, Mahendran O, Krishnaveni K (2003) Effect of CeO_2 on conductivity of PMMA/PEO polymer blend electrolytes. *J New Mater Electrochem Syst* 6:25–28
- Yusof YM, Kadir MFZ (2016) Electrochemical characterizations and the effect of glycerol in biopolymer electrolytes based on methylcellulose-potato starch blend. *Mol Cryst Liq Cryst* 627: 220–233
- Shuhaimi NEA, Teo LP, Woo HJ, Majid SR, Arof AK (2012) Electrical double-layer capacitors with plasticized polymer electrolyte based on methyl cellulose. *Polym Bull* 69:807–826
- Yusof YM, Majid A, Kasmani M, Illias HA, Kadir MFZ (2014) The effect of plasticization on conductivity and other properties of starch/chitosan blend biopolymer electrolyte incorporated with ammonium iodide. *Mol Cryst Liq Cryst* 603:73–88
- Tuhin MO, Rahman N, Haque M, Khan RA, Dafader N, Islam R, Numabi M, Tonny W (2012) Modification of mechanical and thermal property of chitosan-starch blend films. *Radiat Phys Chem* 81: 1659–1688
- Shukur M, Ithnin R, Kadir MFZ (2014) Electrical characterization of corn starch-LiOAc electrolytes and application in electrochemical double layer capacitor. *Electrochim Acta* 136:204–216
- Noor S, Ahmad A, Talib I, Rahman M (2011) Effect of ZnO nanoparticles filler concentration on the properties of PEO-ENR50-LiCF₃SO₃ solid polymeric electrolyte. *Ionics* 17:451–456
- Salunkhe RR, Tang J, Kamachi Y, Nakato T, Kim JH, Yamauchi Y (2015) Asymmetric supercapacitors using 3D nanoporous carbon and cobalt oxide electrodes synthesized from a single metal-organic framework. *ACS Nano* 23:6288–6296
- Wang C, Wallace GG (2015) Flexible electrodes and electrolytes for energy storage. *Electrochim Acta* 175:87–95
- Vijayakumar S, Nagamuthu S, Muralidharan G (2013) Supercapacitor studies on NiO nanoflakes synthesized through a microwave route. *ACS Appl Mater Interfaces* 5:2188–2196
- Duraisamy N, Numan A, Fatin SO, Ramesh K, Ramesh S (2016) Facile sonochemical synthesis of nanostructured NiO with different particle sizes and its electrochemical properties for supercapacitor application. *J Colloid Interface Sci* 471:136–144
- Yusof YM (2017) Characteristics of corn starch/chitosan blend green polymer electrolytes complexed with ammonium iodide and its application in energy devices. PhD Dissertation, University of Malaya
- Arof A, Shuhaimi N, Alias N, Kufian M, Majid S (2010) Application of chitosan/iota-carrageenan polymer electrolytes in electrical double layer capacitor (EDLC). *J Solid State Electrochem* 14:2145–2152
- Burke A, Yilmaz E, Hasirci N, Yilmaz O (2002) Iron (III) ion removal from solution through adsorption on chitosan. *J Appl Polym Sci* 84:1185–1192
- Arof AK, Amirudin S, Yusof SZ, Noor IM (2014) A method based on impedance spectroscopy to determine transport properties of polymer electrolytes. *Phys Chem Chem Phys* 16:1856–1867
- Rice MJ, Roth WL (1972) Ionic transport in super ionic conductors: a theoretical model. *J Solid State Chem* 4:294–310
- Wagner JB, Wagner CJ (1957) Electrical conductivity measurements on cuprous halides. *J Chem Phys* 26:1597–1601
- Samsudin AS, Khairul WM, Isa MIN (2012) Characterization on the potential of carboxy methylcellulose for application as proton conducting biopolymer electrolytes. *J Non-Cryst Solids* 358:1104–1112
- Malathi J, Kumaravadivel M, Brahmanandhan GM, Hema M, Baskaran R, Selvasekarapandian S (2010) Structural, thermal and electrical properties of PVA-LiCF₃SO₃ polymer electrolyte. *J Non-Cryst Solids* 356:2277–2281
- Stephan AM, Thirunakaran R, Renganathan NG, Sundaram V, Pitchumani G, Muniyandi N, Gangadharan R, Ramamoorthy P (1999) A study on polymer blend electrolyte based on PVC/PMMA with lithium salt. *J Power Sources* 81–82:752
- Kartha SA (2013) A preparation of B₂O₃-Li₂O-MO (M = Pb, Zn) glass thin films and study of thin properties. Dissertation, Mahatma Gandhi University
- Hema M, Selvasekarapandian S, Sakunthala A, Arunkumar D, Nithya H (2008) Structural, vibrational and electrical characterization of PVA-NH₄Br polymer electrolyte system. *Physica B* 403: 2740–2747
- Kim DW, Kim YR, Park JK, Moon SI (1998) Electrical properties of the plasticized polymer electrolytes based on acrylonitrile-methyl methacrylate copolymers. *Solid State Ionics* 106:329–337
- Selvasekarapandian S, Baskaran R, Hema M (2005) Complex AC impedance, transference number and vibrational spectroscopy studies of proton conducting PVAc-NH₄SCN polymer electrolytes. *Physica B* 357:412–419
- Khair AS, Arof AK (2010) Conductivity studies of starch-based polymer electrolytes. *Ionics* 16:123–129
- Richardson S, Gorton L (2003) Characterisation of the substituent distribution in starch and cellulose derivatives. *Anal Chim Acta* 497:27–65
- Fadzallah IA, Noor IM, Careem MA, Arof AK (2016) Investigation of transport properties of chitosan-based electrolytes utilizing impedance spectroscopy. *Ionics* 22:1635–1645
- Noor ISM (2016) Characterization and transport properties of PVA-LiBOB based polymer electrolytes with application in dye sensitized solar cells, PhD Dissertation, University of Malaya
- Shamsuddin L, Noor LM, Albinsson I, Mellander BE, Arof AK (2017) Perovskite solar cells using polymer electrolytes. *Mol Cryst Liq Cryst* 655:181–194
- Shukur MF, Ithnin R, Kadir MFZ (2014) Electrical properties of proton conducting solid biopolymer electrolytes based on starch-chitosan blend. *Ionics* 20:977–999
- Kufian MZ, Aziz MF, Shukur MF, Rahim AS, Ariffin NE, Shuhaimi NEA, Majid SR, Yahya R, Arof AK (2012) PMMA-LiBOB gel electrolyte for application in lithium ion batteries. *Solid State Ionics* 208:36–42

35. Nadimicherla R, Kalla R, Muchakayala R, Guo X (2015) Effect of potassium iodide (KI) on crystallinity, thermal stability, and electrical properties of polymer blend electrolytes (PVC/PEO: KI). *Solid State Ionics* 278:260–267
36. Hu X, Muchakayala R, Song S, Wang J, Chen J, Tan M (2018) Synthesis and optimization of new polymeric ionic liquid poly(diallyldimethylammonium) bis(trifluoromethane sulfonyl)imide based gel electrolyte films. *Int J Hydrog Energy* 43:3741–3749
37. Jinisha B, Anilkumar KM, Manoj M, Pradeep VS, Jayalekshmi S (2017) Development of a novel type of solid polymer electrolyte for solid state lithium battery applications based on lithium enriched poly(ethylene oxide) (PEO)/poly(vinyl pyrrolidone) (PVP) blend polymer. *Electrochim Acta* 235:210–222
38. Woo HJ, Majid SR, Arof AK (2011) Transference number and structural analysis of proton conducting polymer electrolyte based on poly(ϵ -caprolactone). *Mater Res Innov* 15:S49–S54
39. Kadir MFZ, Arof AK (2011) Application of PVA-chitosan blend polymer electrolyte membrane in electrical double layer capacitor. *Mater Res Innov* 15:S217–S220
40. Pandey GP, Hashmi SA (2013) Ionic liquid 1-ethyl-3-methylimidazolium tetracyanoborate-based gel polymer electrolyte for electrochemical capacitors. *J Mater Chem A* 1:3372–3378
41. Muchakayala R, Song S, Wang J, Faa Y, Benggeppagari M, Chen J, Tan M (2018) Development and supercapacitor application of ionic liquid-incorporated gel polymer electrolyte films. *J Ind Eng Chem* 59:79–89
42. Nasibi M, Golozar MA, Rashed G (2012) Nano zirconium oxide/carbon black as a new electrode material for electrochemical double layer capacitors. *J Power Sources* 206:108–110
43. Wang X, Li W, Wang X, Zhang J, Sun L, Gao C, Shang J, Hu Y, Zhu Q (2017) Electrochemical properties of NiCoO₂ synthesized by hydrothermal method. *RSC Adv* 7:50753–50759
44. Liew C-W, Ramesh S (2015) Electrical, structural, thermal and electrochemical properties of corn starch-based biopolymer electrolytes. *Carbohydr Polym* 124:222–228
45. Bandaranayake CM, Weerasinghe SS, Vidanapathirana KP, Perera KS (2015) A cyclic voltammetry study of a gel polymer electrolyte based redox-capacitor. *Sri Lankan J Phys* 7:1–11
46. Cui H, Zhu G, Liu X, Liu F, Xie Y, Yang C, Lin T, Gu H, Huang F (2015) Niobium nitride Nb₄N₅ as a new high-performance electrode material for supercapacitors. *Adv Sci* 2:1500126
47. Ranaweera CK, Kahol PK, Ghimire M, Mishra SR, Gupta RK (2017) Orange-peel-derived carbon: designing sustainable and high-performance supercapacitor electrodes. *C* 3:1–17
48. Yang Y, Ruan G, Xiang C, Wang G, Tour JM (2014) Flexible three-dimensional nanoporous metal-based energy devices. *J Am Chem Soc* 136:6187–6190
49. Arof AK, Kufian MZ, Shukur MF, Aziz MF, Abdelrahman AE, Majid SR (2012) Electrical double layer capacitor using poly(methyl methacrylate)-C₄BO₈Li gel polymer electrolyte and carbonaceous material from shells of mata kucing (*Dimocarpus longan*) fruit. *Electrochim Acta* 74:39–45
50. Chen T, Dai L (2013) Carbon nanomaterials for high performance supercapacitors. *Mater Today* 16:272–280
51. Teoh KH, Lim C-S, Liew C-W, Ramesh S, Ramesh S (2015) Electric double-layer capacitors with corn starch-based biopolymer electrolytes incorporating silica as filler. *Ionics* 21:2061–2068
52. Lim C-S, Teoh KH, Liew C-W, Ramesh S (2014) Electric double layer capacitor based on activated carbon electrode and biodegradable composite polymer electrolyte. *Ionics* 20:251–258

Publisher's note Springer Nature remains neutral with regard to jurisdictional claims in published maps and institutional affiliations.